

# Synthesis, characterization of (*R*)-2,2'-diamino-1,1'-binaphthyl mono-sulfonamide and its ruthenium complex and evaluation of the catalytic properties in transfer hydrogenation reactions

Lisheng Cai \*, Ying Han, Hussein Mahmoud, Brent M. Segal <sup>1</sup>

*The Department of Chemistry, The University of Illinois at Chicago, Chicago, IL 60607, USA*

Received 19 February 1998; received in revised form 22 May 1998

## Abstract

(*R*)-2-amino-2'-(8-quinolinesulfonyl amino)-1,1'-binaphthyl is synthesized. Its ruthenium complex is shown to be an asymmetric catalyst for transfer hydrogenation reactions in high chemical yield and modest enantioselectivity. Single crystal diffraction studies of both the ligand and the ruthenium complex show strong  $\pi$ -stacking interactions between the quinoline ring and one of the naphthyl groups. The relationship between the structure and catalytic reactivity is also discussed. © 1998 Elsevier Science S.A. All rights reserved.

**Keywords:** Asymmetric; Ruthenium; Sulfonamide; Binaphthyl; Transfer hydrogenation

## 1. Introduction

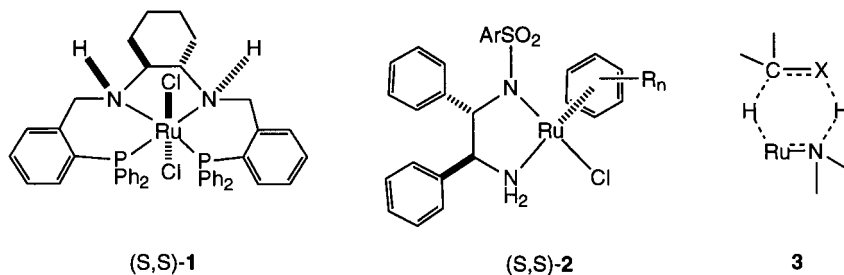
Asymmetric reduction of C=O and C=N bonds forming chiral alcohols and amines, respectively, is among the most fundamental molecular transformations [1]. In nature, oxidoreductases, such as horse liver alcohol dehydrogenase, catalyze transfer hydrogenation of carbonyl compounds to alcohols using cofactors like NADH or NADPH [2]. Such biochemical reactions are normally very stereoselective. However, organic synthesis needs economically and technically more beneficial methods that are very general. A reaction using non-hazardous organic molecules provides a useful complement to catalytic reduction using molecular hydrogen, particularly for small to medium scale reactions. Transfer hydrogenation is operationally simple, and the selectivities including functional group differentiation may be different from those of hydrogenation. Catalytic

asymmetric transfer hydrogenation has remained quite primitive [3]. It is only recently that some successful examples have been reported for the reduction of some activated olefins, aromatic ketones, and imines using alcohols or formic acid as the hydrogen source [4]. Two of the successful examples of the catalysts are shown in Scheme 1.

A number of features have been discovered for these series of catalysts: (a) the ligands accelerate the reaction; (2) two equivalents of KOH are needed per catalyst; (3) the presence of an NH moiety in each ligand is crucially important. A mechanistic model based on these observations has been proposed. Some of the key features are that the hydrogen transfer occurs via metal–ligand bifunctional catalysis, and the NH linkage can stabilize a transition state by forming a hydrogen bond with the heteroatom. The six-membered cyclic transition structure is schematically visualized by **3** in Scheme 1. Scheme 2 illustrates the general sense of asymmetric induction in transfer hydrogenation of imines and aromatic ketones for one of the catalysts. Here we want to report our initial efforts in this area of research.

\* Corresponding author. Tel.: +1 312 9963161; fax: +1 312 9960431; e-mail: cai@uic.edu

<sup>1</sup> Present address: Department of Chemistry and Chemical Biology, Harvard University, 12 Oxford Street, Cambridge, MA 02138, USA.



Scheme 1. Some examples of catalysts for transfer hydrogenations and proposed key intermediate or transition state ( $X = O, NR$ ).

## 2. Results and discussion

Compared with the asymmetric ligands based on BINAP and 1,1'-bi-2-naphthol [5], asymmetric ligands based on 1,1'-binaphthyl-2,2'-diamine, 1,1'-binaphthyl-2-amino-2'-hydroxy, and 1,1'-binaphthyl-2-amino-2'-thiol, are scarce [6]. However, promising results have been obtained in the catalysis of Mukaiyama reactions [7].

### 2.1. Synthesis of the ligand

We set out to explore the asymmetric induction based on the last three categories of 1,1'-binaphthyl compounds. The synthesis of 8-quinolinesulfonyl amide **5** is shown in Scheme 3. Multiple trials, to select an optimal condition to synthesize the sulfonamide, result in finding that the reaction works best in a dilute solution of acetonitrile with pyridine as base (8-quinoline sulfonyl chloride is not very soluble in  $CH_3CN$ ). The most common problem is the precipitate formation between 2,2'-diamine-1,1'-binaphthyl or pyridine and 8-quinolinesulfonyl chloride in other solvents. Reactions of sulfonyl chlorides and amines in DMF result in our discovery of a new procedure for the synthesis of formamidines [8].

X-ray quality crystals for compound **5** were grown from  $CH_3CN/Et_2O$ . The results of this study are shown in Fig. 1 and Tables 1–3. The bond angle around the

sulfonyl amide ( $C12-N2-S1$ ) is  $124^\circ$ , typical for *N*-arylsulphonamides, where the nitrogen is  $sp^2$  hybridized [9]. The other bond distances and bond angles for each individual atom for this molecule are within the range for these types of compounds.

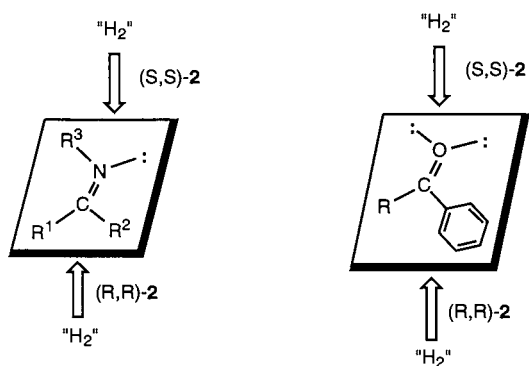
However, the arrangement of groups within the molecule is quite interesting. The quinoline ring and one of the naphthyl rings are slightly tilted toward each other with a dihedral angle of  $5.2^\circ$ . The interplanar distance is about  $3.3 \text{ \AA}$ , which closely matches that of the graphite and other  $\pi$ -stacking systems. Importantly,  $\pi$ -stacking may not be the only interaction to keep the two rings close and parallel. We believe that they may also interact through  $\pi$ -donor and  $\pi$ -acceptor bonds. The quinoline ring is electronically poor and can act as an electron acceptor, while the naphthyl group with amine or amide substituent attached may act as an electron donor. The magnitude of this interaction is also reflected in the formation of the transition metal complex as described below. The dihedral angle between the naphthyl rings toward the two nitrogen atoms is  $83^\circ$ , as compared with  $86^\circ$  in 1,1'-binaphthyl-2-amino-2'-hydroxy [10].

### 2.2. Catalytic reactivity of the ligand **5** for a number of *in situ* reactions

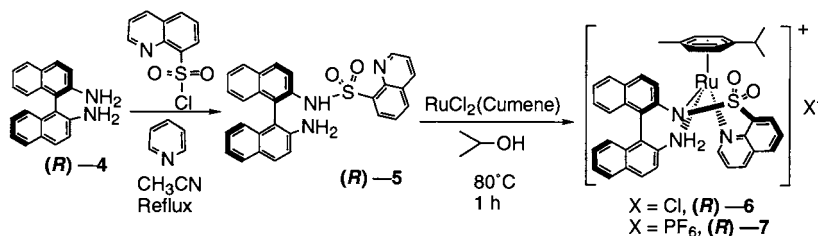
No catalytic activity is observed for the reaction between  $Zn(C_2H_5)_2$  and aldehydes such as benzaldehyde ( $PhCHO$ ) and *trans*- $PhCH=CHCHO$ . Pre-mixing of **5** with  $Ti(OPr^i)_4$  did not improve the reaction. Cyclopropanation of styrene with ethyl diazoacetate in the presence of the ligand **5** and  $CuOTf$  generates ethyl 1-phenyl-1-cyclopropanecarboxylate in high chemical yield, however, no e.e. is observed.

### 2.3. Synthesis of the complex **6**

The reaction of ligand **5** with  $RuCl_2(\text{Cumene})$  in refluxing 2-isopropanol generates a half sandwich complex **6**. The complex is soluble in most common organic solvents such as THF, ether, methanol, ethanol,  $CH_2Cl_2$ ,  $CHCl_3$ , and slightly soluble in  $CH_3CN$ , toluene, benzene. Exchange of the anion chloride in **6**



Scheme 2. General sense of selectivity by one of the asymmetric transfer hydrogenation catalysts.

Scheme 3. Synthesis of ligand **5** and its ruthenium complex **6**.

by  $\text{AgPF}_6$  generates **7** (Scheme 3), showing that the chloride is not in the immediate coordination sphere of ruthenium. Other ruthenium starting materials such as norbornene ruthenium dichloride or ruthenium trichloride do not generate any complexes. The free ligand is un-changed under a variety of conditions such as different solvents (DMF, isopropanol), and temperatures (r.t. to  $150^\circ\text{C}$ ).

#### 2.4. Structure of the complex **6**

Crystals suitable for X-ray single crystal study were grown from  $\text{CH}_3\text{CN}/\text{Et}_2\text{O}$  system as detailed in the experimental section. Two similar molecules exist in each asymmetric unit. Structural information for only one of them is given in Fig. 2 and Tables 4–6. The ruthenium is a saturated diamagnetic 18-electron center. The  $\eta^6$ -coordination of the cumene is maintained with an average distance of  $2.20 \pm 0.04 \text{ \AA}$ , comparable with that of the neutral analog [11]. While the bond lengths of Ru–amide (Ru–N2) and Ru–quinoline (Ru–N3) are comparable with other Ru–analogs [11], the Ru–amine (Ru–N1) bond is longer by  $0.1 \text{ \AA}$ . This may be the bond broken when the ruthenium center opens its coordination for substrate binding. The dihedral angle between the two naphthyl rings toward the two nitrogen atoms is  $71^\circ$ , reduced from  $83^\circ$  in free ligand **5**. The bond angles around N2 are almost unchanged as compared with free ligand,  $120 \pm 2^\circ$ . Overlap of the structure of the complex **6** with that of its free ligand **5** reveals minor changes in the ligand portion, except for the decrease of the dihedral angle between the two naphthyl rings toward the ruthenium center. The dihedral angle of the quinoline ring, and one of the naphthyl rings, is  $9.1^\circ$ , only slightly larger than  $5.2^\circ$  observed in free ligand **5**. It appears that the ligand has a strong tendency to maintain its own structure even after it coordinates with the transition metal fragment. Amazingly, the ruthenium complex is the only one we can make out of this ligand up to now. This may mean that only the metal fragment, which matches the geometric requirements of this multidentate ligand, can coordinate. Substitution of the amino-group  $\text{NH}_2$  with a hydroxy group  $\text{OH}$  prevents formation of the ruthenium complex at a variety of conditions [12].

#### 2.5. Catalytic reactivity of the complex for transfer hydrogenations

As a start, ruthenium complex **6** (Scheme 4) catalyzes the transfer hydrogenations of ketones in isopropanol at  $80^\circ\text{C}$  to give the corresponding alcohols in high yield, but with modest enantioselectivity at best. It seems that the reduced reactivity of this complex comes from the lack of an empty coordination site at r.t. The most probable pre-dissociation is the weak ruthenium–amine bond, which may reduce the influence of the chiral center on the incoming ketones or imines. The presence of a base such as  $\text{Na}_2\text{CO}_3$  destroys the catalyst, no reaction is observed in isopropanol at  $80^\circ\text{C}$  overnight. No intermediates were observed during the reaction by  $^1\text{H-NMR}$ . After the reaction, the catalyst was recovered at 92%.

Transfer hydrogenation of  $\alpha,\beta$ -unsaturated aldehydes or ketones such as chalone (*trans*- $\text{PhCH}=\text{CHCOPh}$ ) generates a mixture of products which originate from either C=C bond, or C=O bond, or simultaneous reduction of C=C and C=O bonds. Stronger reducing agents such as formic acid and triethylamine generate similar results under the same conditions. However, no difference in e.e. values is observed. Lowering temperature dramatically slows down the reactions.  $\alpha,\beta$ -Unsaturated acids or esters such as methyl cinnamic ester (*trans*- $\text{PhCH}=\text{CHCOOCH}_3$ ) or  $\beta$ -methyl cinnamic acid (*trans*- $\text{Ph(Me)C}=\text{CHCOOH}$ ) cannot be reduced under the same conditions. No reduction is observed for imines such as *trans*- $\text{Ph(Me)C}=\text{N-Ph}$ .

#### 2.6. Mechanistic implication

Since **6** and **7** are both 18-electron ruthenium complexes, the catalysis may begin by predissociation of one of the coordination sites. The ruthenium–amine bond is longer or maybe weaker than the other two ruthenium–nitrogen bonds, and it is the most probable bond to break before the catalyst coordinates with the substrate. Since the chirality of the ligand comes from the chiral axis of the molecule, pre-dissociation of the Ru–amine bond would make the catalyst lose its chiral induction in the transfer hydrogenations. It may ac-

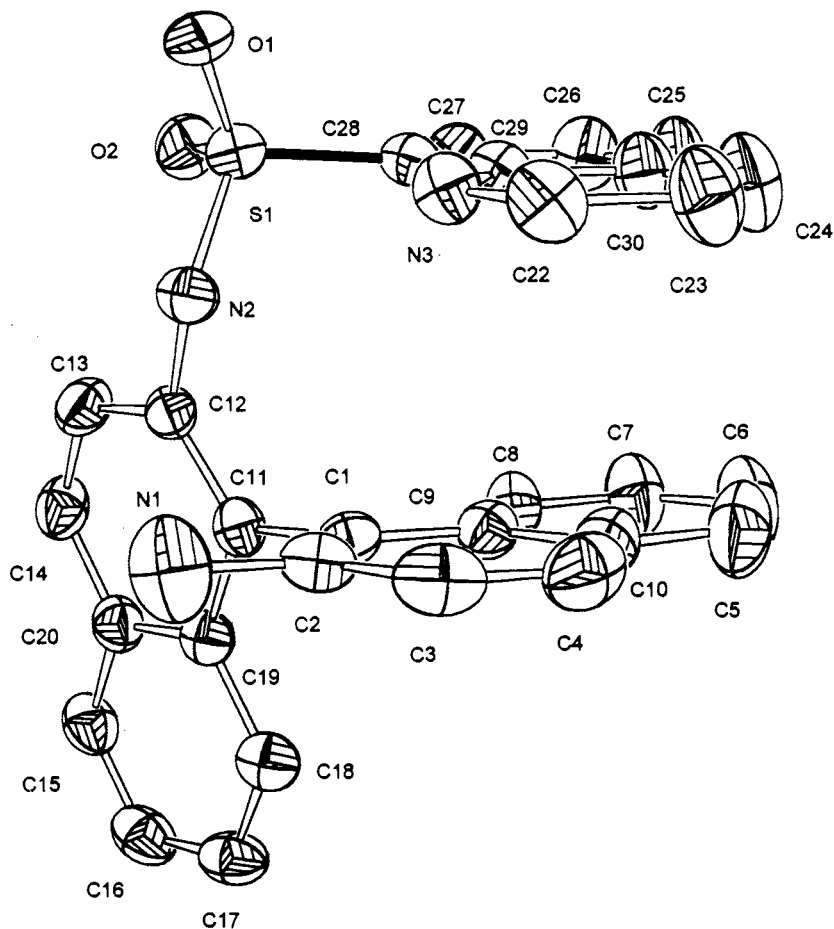


Fig. 1. Molecular structure of ligand **5** with atomic numbering (ORTEP, 50% probability ellipsoids, hydrogen atoms omitted for clarity).

count for the low chiral induction of the reductions. The Ru–amine bond is also difficult to break, and it may be the reason that a high temperature is needed for the catalysts to be functional.

### 2.7. Catalytic reactivity of the complex **6** for other reactions

Other hydrogen sources, such as  $H_2$  and  $NaBH_4$ , have been tested for the reduction of ketones and  $\alpha,\beta$ -unsaturated aldehydes or ketones. The former reagent gives no product, and no change in catalyst is observed. The latter in methanol destroys the catalyst, free ligand is observed as checked by TLC.

### 3. Conclusion

We have described a ligand based on the monosulfonamide of 2,2'-diamine-1,1'-binaphthyl and its complex with ruthenium(II). The ligand has a strong tendency to retain its original configuration. Evaluation of the catalytic properties of both the free ligand under in situ conditions and its ruthenium complex has been described.

It was discovered that the ruthenium complex catalyzes the transfer hydrogenations between ketones and isopropanol at  $80^\circ C$ . The reaction gives high chemical yield, but only modest enantioselectivity is observed. The general harsh conditions needed to open one coordination site for the reaction, probably the dissociation of the amino group, may render the reactive intermediate less selective toward the substrates.

### 4. Experimental

#### 4.1. General considerations

(*R*)-(+)-2,2'-diamine-1,1'-binaphthyl, 8-quinolinesulfonyl chloride, and  $[RuCl_2(\eta^6\text{-cumene})_2]$  were purchased from Aldrich. All manipulations were carried out using either high-vacuum or glovebox techniques.  $^1H$ - and  $^{13}C$ -NMR spectra were recorded on a Bruker AMX-400 spectrometer at 400.1 and 100.6 MHz, a Bruker AMX-200 spectrometer at 200.1 MHz, or Varian 300 spectrometer at 299.949 MHz and 75.429 MHz, respectively. Enantioselectivity (e. e.) was measured on Chiralcel-OD column at 254 nm with isopropanol/hexane (5:95) as eluents.

## 4.2. Ligand 5

(R)-(+) -2,2'-diamine-1,1'-binaphthyl (120 mg, 0.423

Table 1  
Crystal data and structure refinement for 5

Crystal data	
Empirical formula	C <sub>29</sub> H <sub>21</sub> N <sub>3</sub> O <sub>2</sub> S · CH <sub>3</sub> CN
Crystal habit	White
Crystal system	Monoclinic
Space group	<i>P</i> 2(1)/ <i>n</i>
Unit cell dimensions	
<i>a</i> (Å)	14.1083 (10)
<i>b</i> (Å)	13.2949 (10)
<i>c</i> (Å)	14.8700 (11)
$\beta$ (°)	113.6460 (10)
Volume (Å <sup>3</sup> )	2555.0 (3)
<i>Z</i>	4
Formula weight	516.60
<i>D</i> <sub>calc</sub> (Mg m <sup>-3</sup> )	1.343
Absorption coefficient (mm <sup>-1</sup> )	0.164
<i>F</i> (000)	1080
Data collection	
Diffractionmeter used	Siemens SMART/CCD
Radiation (Å)	0.71073
Temperature (K)	213(2)
2 $\theta$ Range	3.36 < 2 $\theta$ < 45.00
Scan speed (° min <sup>-1</sup> )	1.2 in $\omega$
Index range	-12 ≤ <i>h</i> ≤ 18, -17 ≤ <i>k</i> ≤ 17, -19 ≤ <i>l</i> ≤ 15
Total reflections	10 585
Independent reflections	3339 [ <i>R</i> <sub>int</sub> = 0.0595]
Solution and refinement	
System used	Shelx 93
Solution	Direct methods
Refinement method	Full-matrix least-squares on <i>F</i> <sup>2</sup>
Weighting scheme	$\omega^{-1} = \sigma^2(F_o^2) + (0.0553P)^2 + 0.93(P)$
	$P = [\max(F_o^2, 0) + 2(F_c^2)]/3$
Final <i>R</i> Indices [ <i>I</i> > 2 $\sigma$ ( <i>I</i> )]	<i>R</i> <sub>1</sub> = 0.0530
	$R_1 = \Sigma \ F_o\  -  F_c  / \Sigma  F_o $
	$wR_2 = 0.1093$ , where $wR_2 = \{\Sigma [w(F_o^2 - F_c^2)^2] / \Sigma [w(F_o^2)^2]\}^{1/2}$
<i>R</i> Indices (all data)	<i>R</i> <sub>1</sub> = 0.0974, <i>wR</i> <sub>2</sub> = 0.1321
Goodness-of-fit on <i>F</i> <sup>2</sup>	1.054, where GOF = $[\Sigma [w(F_o^2 - F_c^2)^2] / (n - p)]^{1/2}$ and <i>n</i> and <i>p</i> denotes the number of data and parameters.
Data/restraints/parameters	3336/0/344
Maximum and minimum	
Difference peaks (e Å <sup>-3</sup> )	0.332 and -0.345

Table 2

Atomic coordinates (×10<sup>4</sup>) and equivalent isotropic displacement parameters (Å<sup>2</sup> × 10<sup>3</sup>) for 5

Atom	<i>x</i>	<i>y</i>	<i>z</i>	<i>U</i> <sub>eq</sub>
S(1)	8511(1)	5503(1)	1757(1)	37(1)
O(1)	9497(2)	5998(2)	2115(2)	45(1)
O(2)	8158(2)	5075(2)	2452(2)	45(1)
N(1)	8958(2)	3688(3)	-911(3)	61(1)
N(2)	8568(2)	4611(2)	1020(2)	35(1)
C(1)	7307(3)	4299(3)	-1025(2)	33(1)
C(2)	8112(3)	4307(3)	-1330(3)	37(1)
C(3)	8085(3)	4975(3)	-2082(3)	46(1)
C(4)	7282(3)	5607(3)	-2509(3)	52(1)
C(5)	5625(4)	6337(3)	-2612(3)	67(1)
C(6)	4837(4)	6369(3)	-2301(4)	73(2)
C(7)	4834(3)	5702(3)	-1573(3)	58(1)
C(8)	5622(3)	5025(3)	-1165(3)	43(1)
C(9)	6457(3)	4976(3)	-1461(3)	36(1)
C(10)	6442(3)	5645(3)	-2213(3)	47(1)
C(11)	7310(2)	3586(2)	-250(3)	31(1)
C(12)	7880(2)	3767(2)	732(3)	31(1)
C(13)	7841(3)	3106(3)	1461(3)	41(1)
C(14)	7261(3)	2258(3)	1199(3)	42(1)
C(15)	6154(3)	1079(3)	-76(3)	43(1)
C(16)	5634(3)	839(3)	-1041(3)	46(1)
C(17)	5636(3)	1509(3)	-1773(3)	42(1)
C(18)	6166(3)	2402(3)	-1525(3)	37(1)
C(19)	6731(2)	2666(3)	-528(3)	31(1)
C(20)	6707(3)	1990(3)	204(3)	36(1)
N(3)	8508(2)	6619(2)	12(2)	39(1)
C(22)	8594(3)	7109(3)	-723(3)	47(1)
C(23)	7905(3)	7860(3)	-1271(3)	55(1)
C(24)	7072(3)	8081(3)	-1074(3)	57(1)
C(25)	6082(3)	7755(3)	-57(3)	55(1)
C(26)	5968(3)	7239(3)	684(3)	50(1)
C(27)	6713(3)	6529(3)	1225(3)	41(1)
C(28)	7554(3)	6355(3)	1016(3)	34(1)
C(29)	7689(3)	6862(3)	236(3)	36(1)
C(30)	6932(3)	7580(3)	-304(3)	42(1)
N(1S)	9348(5)	1682(4)	374(7)	178(3)
C(1S)	9059(4)	957(5)	445(4)	80(2)
C(2S)	8646(5)	8(5)	473(6)	156(3)

*U*<sub>eq</sub> is defined as one third of the trace of the orthogonalized *U*<sub>*ij*</sub> tensor.

mmol) and 8-quinolinesulfonyl chloride (110 mg, 0.486 mmol) were dissolved in 120 ml dried acetonitrile under nitrogen. Pyridine (0.2 ml) was then added into the flask. The reaction mixture was refluxed overnight or until the reaction was finished as checked by TLC. After the reaction, silica gel (1–2 g) was added into the flask. The solvent was removed. The product was isolated by column chromatography with hexane/ethyl acetate (3:1) as eluant to afford 193 mg product. Yield 96%. <sup>1</sup>H-NMR (CD<sub>3</sub>CN at 400 MHz),  $\delta$ , 8.55 (brs, 1H, amide NH); 8.13–8.02 (m, 5H, Ar-H); 7.92 (d, <sup>3</sup>*J*<sub>HH</sub> = 8.2 Hz, 1H, Ar-H); 7.86 (dd, <sup>3</sup>*J*<sub>HH</sub> = 8.2 Hz, <sup>4</sup>*J*<sub>HH</sub> = 1.2 Hz, 1H, Ar-H); 7.48–7.36 (m, 4H, Ar-H); 7.31 (dd, <sup>3</sup>*J*<sub>HH</sub> = 8.2 Hz, <sup>3</sup>*J*<sub>HH</sub> = 4.3 Hz, 1H, Ar-H); 7.15 (ddd,

$^3J_{\text{HH}} = 8.3$  Hz,  $^3J_{\text{HH}} = 9.8$  Hz,  $^4J_{\text{HH}} = 1.1$  Hz, 1H, Ar-H); 6.94 (ddd,  $^3J_{\text{HH}} = 7.1$  Hz,  $^3J_{\text{HH}} = 8.1$  Hz,  $^4J_{\text{HH}} = 1.0$  Hz, 1H, Ar-H); 6.82 (d,  $^3J_{\text{HH}} = 8.8$  Hz, 1H, Ar-H); 6.74 (d,  $^3J_{\text{HH}} = 8.8$  Hz, 1H, Ar-H); 6.61 (ddd,  $^3J_{\text{HH}} = 7.0$  Hz,  $^3J_{\text{HH}} = 8.2$  Hz, 1H, Ar-H); 6.03 (d,  $^3J_{\text{HH}} = 8.3$  Hz, 1H, Ar-H); 3.80 (brs, 2H, NH<sub>2</sub>).  $^{13}\text{C}\{^1\text{H}\}$ - (DMSO-*d*<sub>6</sub> at 300 MHz),  $\delta$ , 185.3; 151.1; 145.1; 142.3; 137.0; 136.5; 135.2; 134.9; 134.4; 133.2; 132.0; 130.6;

129.7; 129.4; 128.8; 128.6; 128.4; 127.3; 126.7; 126.2; 125.9; 125.7; 124.2; 123.4; 123.0; 122.2; 121.5; 118.8; 108.5. GCMS, 475 (35%, M<sup>+</sup>); 458 (5%, M-NH<sub>3</sub><sup>+</sup>); 283 (45%, M-SO<sub>2</sub>Q<sup>+</sup>); 267 (100%, M-NHSO<sub>2</sub>Q<sup>+</sup>); 129 (60%, Q + H<sup>+</sup>). High resolution MS: Found, 475.135898; Calcd, 475.135449530.

Table 3

Bond lengths (Å) and angles (°) for **5**

S(1)–O(2)	1.433(3)	S(1)–O(1)	1.434(2)
S(1)–N(2)	1.639(3)	S(1)–C(28)	1.767(4)
N(1)–C(2)	1.376(4)	N(2)–C(12)	1.432(4)
C(1)–C(2)	1.383(5)	C(1)–C(9)	1.429(5)
C(1)–C(11)	1.490(5)	C(2)–C(3)	1.416(5)
C(3)–C(4)	1.348(5)	C(4)–C(10)	1.421(6)
C(5)–C(6)	1.366(6)	C(5)–C(10)	1.406(6)
C(6)–C(7)	1.400(6)	C(7)–C(8)	1.369(5)
C(8)–C(9)	1.415(5)	C(9)–C(10)	1.422(5)
C(11)–C(12)	1.376(5)	C(11)–C(19)	1.437(5)
C(12)–C(13)	1.415(5)	C(13)–C(14)	1.355(5)
C(14)–C(20)	1.413(5)	C(15)–C(16)	1.362(5)
C(15)–C(20)	1.410(5)	C(16)–C(17)	1.407(5)
C(17)–C(18)	1.372(5)	C(18)–C(19)	1.417(5)
C(19)–C(20)	1.423(5)	N(3)–C(22)	1.318(5)
N(3)–C(29)	1.365(4)	C(22)–C(23)	1.404(5)
C(23)–C(24)	1.353(5)	C(24)–C(30)	1.406(5)
C(25)–C(26)	1.361(5)	C(25)–C(30)	1.406(5)
C(26)–C(27)	1.401(5)	C(27)–C(28)	1.363(5)
C(28)–C(29)	1.418(5)	C(29)–C(30)	1.418(5)
N(1S)–C(1S)	1.068(6)	C(1S)–C(2S)	1.398(7)
O(2)–S(1)–O(1)	118.7(2)	O(2)–S(1)–N(2)	108.6(2)
O(1)–S(1)–N(2)	106.3(2)	O(2)–S(1)–C(28)	107.7(2)
O(1)–S(1)–C(28)	108.8(2)	N(2)–S(1)–C(28)	106.0(2)
C(12)–N(2)–S(1)	124.0(2)	C(2)–C(1)–C(9)	119.7(3)
C(2)–C(1)–C(11)	120.7(3)	C(9)–C(1)–C(11)	119.6(3)
N(1)–C(2)–C(1)	121.7(3)	N(1)–C(2)–C(3)	118.4(3)
C(1)–C(2)–C(3)	119.9(3)	C(4)–C(3)–C(2)	120.9(4)
C(3)–C(4)–C(10)	121.7(4)	C(6)–C(5)–C(10)	121.2(4)
C(5)–C(6)–C(7)	119.8(4)	C(8)–C(7)–C(6)	120.3(4)
C(7)–C(8)–C(9)	121.5(4)	C(8)–C(9)–C(10)	117.6(3)
C(8)–C(9)–C(1)	122.7(3)	C(10)–C(9)–C(1)	119.8(3)
C(5)–C(10)–C(4)	122.5(4)	C(5)–C(10)–C(9)	119.5(4)
C(4)–C(10)–C(9)	118.0(4)	C(12)–C(11)–C(19)	118.5(3)
C(12)–C(11)–C(1)	121.9(3)	C(19)–C(11)–C(1)	119.6(3)
C(11)–C(12)–C(13)	121.3(3)	C(11)–C(12)–N(2)	119.5(3)
C(13)–C(12)–N(2)	119.2(3)	C(14)–C(13)–C(12)	120.1(3)
C(13)–C(14)–C(20)	121.9(4)	C(16)–C(15)–C(20)	120.9(4)
C(15)–C(16)–C(17)	119.9(4)	C(18)–C(17)–C(16)	120.7(4)
C(17)–C(18)–C(19)	120.8(4)	C(18)–C(19)–C(20)	118.0(3)
C(18)–C(19)–C(11)	121.9(3)	C(20)–C(19)–C(11)	120.1(3)
C(15)–C(20)–C(14)	122.3(4)	C(15)–C(20)–C(19)	119.7(3)
C(14)–C(20)–C(19)	118.0(3)	C(22)–N(3)–C(29)	117.0(3)
N(3)–C(22)–C(23)	124.1(4)	C(24)–C(23)–C(22)	119.2(4)
C(23)–C(24)–C(30)	119.5(4)	C(26)–C(25)–C(30)	121.2(4)
C(25)–C(26)–C(27)	120.0(4)	C(28)–C(27)–C(26)	120.3(4)
C(27)–C(28)–C(29)	121.3(3)	C(27)–C(28)–S(1)	119.0(3)
C(29)–C(28)–S(1)	119.7(3)	N(3)–C(29)–C(28)	119.4(3)
N(3)–C(29)–C(30)	122.7(3)	C(28)–C(29)–C(30)	117.8(3)
C(25)–C(30)–C(24)	123.2(4)	C(25)–C(30)–C(29)	119.4(4)
C(24)–C(30)–C(29)	117.4(4)	N(1S)–C(1S)–C(2S)	176.4(8)

#### 4.3. Ruthenium complex **6**

Ligand **5** (500 mg, 1.052 mmol) and [RuCl<sub>2</sub>( $\eta^6$ -cumene)]<sub>2</sub> (354 mg, 0.579 mmol) were dissolved in isopropanol. Triethylamine (3 mmol) was added. The mixture was refluxed at 80°C for 1 h or until the starting material disappeared on TLC plate. The solvent was removed, and the solid was washed with water, to afford product, 738 mg. Recrystallization from methanol/ether gave the product (660 mg).

Alternatively, after the reaction was complete, the solvent was removed under vacuum. The solid was completely dissolved in CH<sub>3</sub>CN. After a few minutes, pure yellow product precipitated out. Yield 92%.

$^1\text{H-NMR}$  (CD<sub>3</sub>OD at 400 MHz),  $\delta$ , 10.31 (d,  $^3J_{\text{HH}} = 5.4$  Hz, 1H, Ar-H); 8.61 (d,  $^3J_{\text{HH}} = 7.5$  Hz, 1H, Ar-H); 8.15 (d,  $^3J_{\text{HH}} = 9.0$  Hz, 1H, Ar-H); 8.06 (d,  $^3J_{\text{HH}} = 8.4$  Hz, 1H, Ar-H); 7.97 (d,  $^3J_{\text{HH}} = 8.1$  Hz, 1H, Ar-H); 7.84 (dd,  $^3J_{\text{HH}} = 5.4$  Hz,  $^3J_{\text{HH}} = 8.4$  Hz, 1H, Ar-H); 7.68 (d,  $^3J_{\text{HH}} = 8.4$  Hz, 1H, Ar-H); 7.42 (t,  $^3J_{\text{HH}} = 7.5$  Hz, 1H, Ar-H); 7.29 (d,  $^3J_{\text{HH}} = 7.5$  Hz, 2H, Ar-H); 7.18 (t,  $^3J_{\text{HH}} = 7.2$  Hz, 1H, Ar-H); 7.11 (t,  $^3J_{\text{HH}} = 7.6$  Hz, 1H, Ar-H); 7.02 (t,  $^3J_{\text{HH}} = 7.6$  Hz, 1H, Ar-H); 6.79 (t,  $^3J_{\text{HH}} = 7.6$  Hz, 1H, Ar-H); 6.63 (dd,  $^3J_{\text{HH}} = 3.9$  Hz,  $^3J_{\text{HH}} = 8.4$  Hz, 3H, Ar-H); 6.24 (d,  $^3J_{\text{HH}} = 6.0$  Hz, 1H, Ar-H); 6.15 (d,  $^3J_{\text{HH}} = 3.6$  Hz, 1H, Ar-H); 6.14 (d,  $^3J_{\text{HH}} = 8.4$  Hz, 1H, Ar-H); 6.03 (d,  $^3J_{\text{HH}} = 6.0$  Hz, 1H, Ar-H); 5.87 (d,  $^3J_{\text{HH}} = 6.0$  Hz, 1H, Ar-H); 2.81 (hepta,  $^3J_{\text{HH}} = 6.9$  Hz, 1H, CH); 2.02 (s, 3H, CH<sub>3</sub>); 1.06 (d,  $^3J_{\text{HH}} = 6.9$  Hz, 3H, CH<sub>3</sub>); 0.89 (d,  $^3J_{\text{HH}} = 6.9$  Hz, 3H, CH<sub>3</sub>).  $^{13}\text{C}\{^1\text{H}\}$ - (DMSO-*d*<sub>6</sub> at 300 MHz),  $\delta$ , 163.9; 144.6; 143.6; 142.9; 137.4; 136.3; 134.9; 134.0; 133.8; 133.6; 132.6; 132.5; 132.1; 131.2; 131.1; 129.3; 128.9; 128.7; 128.2; 127.5; 127.4; 127.1; 126.8; 126.7; 126.5; 126.1; 124.5; 118.7; 118.2; 108.5; 96.3; 96.1; 92.3; 89.6; 85.1; 31.7 (1C, CH); 22.9 (1C, CH<sub>3</sub>); 21.5 (1C, CH<sub>3</sub>); 17.7 (1C, CH<sub>3</sub>). FAB, 710 (22%, M-Cl<sup>+</sup>); 512 (100%, M-Ru(cumene) + H<sup>+</sup>); 385 (77%, M-Ru(cumene)-Q + H<sup>+</sup>). High resolution FAB for C<sub>39</sub>H<sub>34</sub>N<sub>3</sub>O<sub>2</sub>SRu, the cationic portion of the complex: Found, 710.142400; Calcd, 710.141522. Elemental analysis of C<sub>39</sub>H<sub>34</sub>N<sub>3</sub>O<sub>2</sub>SRuCl: Found, C, 61.89; H, 4.56; N, 5.82; Calcd, C, 62.87; H, 4.57; N, 5.63.

#### 4.4. Ruthenium complex **7**

Ruthenium complex **6** was dissolved in acetone. Then AgPF<sub>6</sub> (one equivalent) in acetone was added. A white precipitate came out immediately. After filtering the

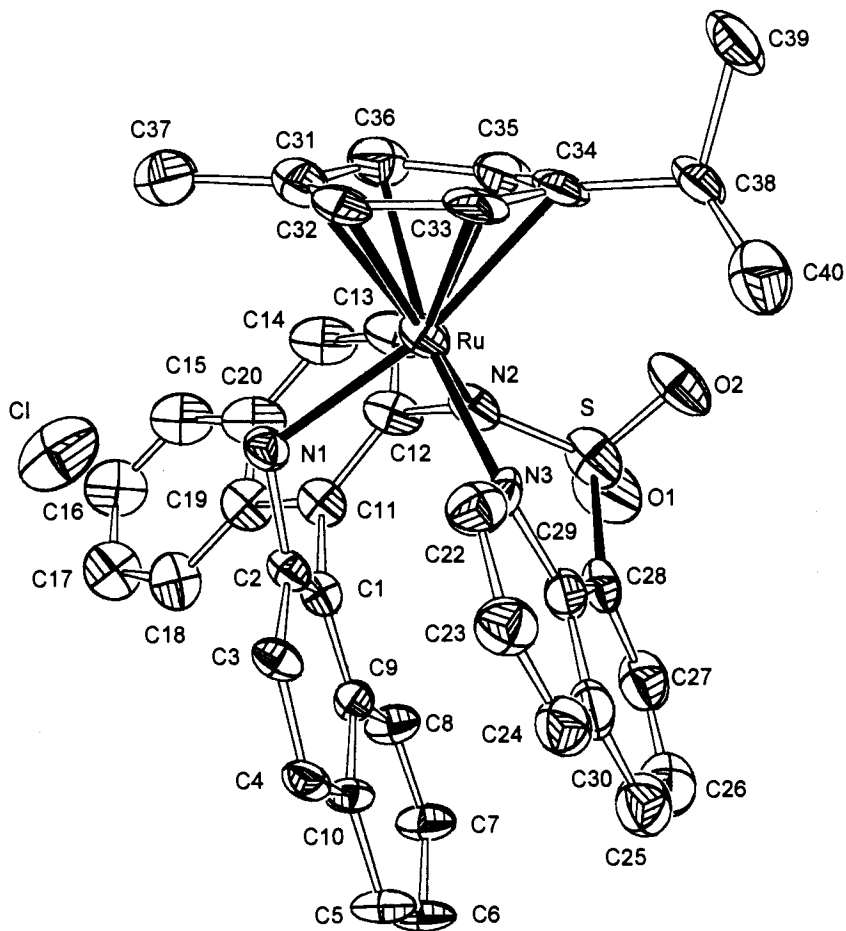


Fig. 2. Molecular structure of the ruthenium complex **6** with atomic numbering (ORTEP, 50% probability ellipsoids, hydrogen atoms omitted for clarity).

solid through celite, the solvent of the clear solution was removed to generate the product **7** with exchanged counterion.  $^1\text{H-NMR}$  (acetone- $d_6$  at 400 MHz),  $\delta$ , 10.6 (d,  $^3J_{\text{HH}} = 5.4$  Hz, 1H, Ar-H); 8.67 (d,  $^3J_{\text{HH}} = 7.5$  Hz, 1H, Ar-H); 8.16 (s, 2H, Ar-H); 8.00 (dd,  $^3J_{\text{HH}} = 8.1$  Hz,  $^4J_{\text{HH}} = 0.9$  Hz, 1H, Ar-H); 7.87 (dd,  $^3J_{\text{HH}} = 5.4$  Hz,  $^3J_{\text{HH}} = 8.1$  Hz, 1H, Ar-H); 7.72 (dd,  $^3J_{\text{HH}} = 8.1$  Hz,  $^4J_{\text{HH}} = 1.8$  Hz, 1H, Ar-H); 7.41 (td,  $^3J_{\text{HH}} = 7.5$  Hz,  $^4J_{\text{HH}} = 1.5$  Hz, 1H, Ar-H); 7.28 (td,  $^3J_{\text{HH}} = 7.2$  Hz,  $^4J_{\text{HH}} = 1.5$  Hz, 2H, Ar-H); 7.18 (td,  $^3J_{\text{HH}} = 7.2$  Hz,  $^4J_{\text{HH}} = 1.5$  Hz, 1H, Ar-H); 7.09 (td,  $^3J_{\text{HH}} = 7.6$  Hz,  $^4J_{\text{HH}} = 1.2$  Hz, 1H, Ar-H); 7.02 (td,  $^3J_{\text{HH}} = 7.6$  Hz,  $^4J_{\text{HH}} = 1.2$  Hz, 1H, Ar-H); 6.79 (t,  $^3J_{\text{HH}} = 7.6$  Hz, 1H, Ar-H); 6.68 (d,  $^3J_{\text{HH}} = 9.0$  Hz, 1H, Ar-H); 6.59 (d,  $^3J_{\text{HH}} = 8.1$  Hz, 1H, Ar-H); 6.52 (d,  $^3J_{\text{HH}} = 8.1$  Hz, 1H, Ar-H); 6.33 (d,  $^3J_{\text{HH}} = 6.0$  Hz, 1H, Ar-H); 6.28 (d,  $^3J_{\text{HH}} = 5.4$  Hz, 1H, Ar-H); 6.18 (d,  $^3J_{\text{HH}} = 8.4$  Hz, 1H, Ar-H); 6.14 (dd,  $^3J_{\text{HH}} = 5.4$  Hz,  $^4J_{\text{HH}} = 0.9$  Hz, 1H, Ar-H); 6.05 (dd,  $^3J_{\text{HH}} = 5.7$  Hz,  $^4J_{\text{HH}} = 0.9$  Hz, 1H, Ar-H); 3.00 (hepta,  $^3J_{\text{HH}} = 6.9$  Hz, 1H, CH); 2.09 (s, 3H,  $\text{CH}_3$ ); 1.06 (d,  $^3J_{\text{HH}} = 6.9$  Hz, 3H,  $\text{CH}_3$ ); 0.89 (d,  $^3J_{\text{HH}} = 6.9$  Hz, 3H,  $\text{CH}_3$ ).

#### 4.5. Catalytic reactions

Typical procedure: acetophenone (12 mg, 0.1 mmol) was dissolved in isopropanol or 1:1 mixture of isopropanol and other solvent (THF, ether, methylene chloride). Ruthenium complex **6** (7 mg, 0.01 mmol) was added. The reaction flask was put in an oil bath at  $80^\circ\text{C}$ . The reaction mixture was refluxed overnight. The solvent was removed, and the product was purified by TLC plate.

For *sec*-phenethyl alcohol,  $^1\text{H-NMR}$  in acetone- $d_6$ , 7.388–7.191 (m, 5H, Ar-H), 4.825 (m, 1H, CH), 4.157 (d, 1H,  $^3J_{\text{HH}} = 4.5$  Hz, OH), 1.383 (d, 3H,  $^3J_{\text{HH}} = 6.6$  Hz,  $\text{CH}_3$ ).

For 1,2,3,4-tetrahydro-1-naphthol,  $^1\text{H-NMR}$  in acetone- $d_6$ , 7.436–7.03 (m, 5H, Ar-H); 4.675 (vt,  $^3J_{\text{HH}} = 4.2$  Hz, 1H, CH); 4.008 (d,  $^3J_{\text{HH}} = 6.0$  Hz, 1H, OH); 2.812–2.702 (m, 2H,  $\text{CH}_2$ ), 2.011–1.942 (m, 2H,  $\text{CH}_2$ ); 1.824–1.707 (m, 2H,  $\text{CH}_2$ ). MS, 148 ( $\text{M}^+$ , 40%), 130 ( $\text{M-H}_2\text{O}^+$ , 100%), 120 ( $\text{M-C}_2\text{H}_4^+$ , 100%), 105 (45%), 91 (80%), 77 (20%).

4.6. Collection and reduction of X-ray data for **5** and **6**

The crystals of **5** were grown from CH<sub>3</sub>CN/ether. For **6**, a number of solvent systems have been tested for generating X-ray quality crystals such as acetone–ether, methanol–ether, acetonitrile–ether, and THF–ether. Poor X-ray quality crystals are generated only in acetonitrile–ether system, only powders are generated in other combinations. Multiple sequential recrystallizations from acetonitrile/ether give crystals enough for single crystal diffraction study.

Table 4  
Crystal data and structure refinement for **6**

Crystal data	
Empirical formula	C <sub>39</sub> H <sub>34</sub> ClN <sub>5</sub> O <sub>2</sub> RuS · 2CH <sub>3</sub> CN
Crystal habit	Yellow
Crystal system	Monoclinic
Space group	<i>P</i> 2(1)
Unit cell dimensions	
<i>a</i> (Å)	9.3025 (5)
<i>b</i> (Å)	38.273 (2)
<i>c</i> (Å)	11.4226 (7)
$\beta$ (°)	108.263 (2)
Volume (Å <sup>3</sup> )	3862.0(4)
<i>Z</i>	4
Formula weight	827.38
<i>D</i> <sub>calc</sub> (Mg m <sup>-3</sup> )	1.423
Absorption coefficient (mm <sup>-1</sup> )	0.573
<i>F</i> (000)	1704
Data collection	
Diffractometer used	Siemens SMART/CCD
Radiation (Å)	0.71073
Temperature (K)	213(2)
2 $\theta$ Range	2.12 < 2 $\theta$ < 48.00
Scan speed (° min <sup>-1</sup> )	1.2 in $\omega$
Index range	-12 ≤ <i>h</i> ≤ 12, -37 ≤ <i>k</i> ≤ 50, -14 ≤ <i>l</i> ≤ 15
Total reflections	19012
Independent reflections	9231 [ <i>R</i> <sub>int</sub> = 0.1579]
Solution and refinement	
System used	Shelx 93
Solution	Direct methods
Refinement method	Full-matrix least-squares on <i>F</i> <sup>2</sup>
Weighting scheme	$\omega^{-1} = \sigma^2(F_o^2) + (0.0523P)^2$ $P = [\max(F_o^2, 0) + 2(F_c^2)]/3$
Final <i>R</i> Indices [ <i>I</i> > 2 $\sigma$ ( <i>I</i> )]	<i>R</i> <sub>1</sub> = 0.0794 $R_1 = \frac{\sum \ F_o\  -  F_c }{\sum  F_o }$ <i>wR</i> <sub>2</sub> = 0.1261, where $wR_2 = \frac{\sum [w(F_o^2 - F_c^2)]}{\sum [w(F_o^2)^2]^{1/2}}$
<i>R</i> indices (all data)	<i>R</i> <sub>1</sub> = 0.1730, <i>wR</i> <sub>2</sub> = 0.1830
Goodness-of-fit on <i>F</i> <sup>2</sup>	0.997, where $GOF = \frac{\sum [w(F_o^2 - F_c^2)^2 / (n - p)]^{1/2}}{\text{number of data and parameters}}$
Data/restraints/parameters	9218/601/960
Maximum and minimum difference peaks (e Å <sup>-3</sup> )	0.757 and -0.707
Absolute structure parameter	0.54(9)

Table 5

Atomic coordinates (×10<sup>4</sup>) and equivalent isotropic displacement parameters (Å<sup>2</sup> × 10<sup>3</sup>) for **6**

Ru(1A)	2194(2)	2921(1)	5507(1)	27(1)
Cl(1A)	3562(5)	3735(1)	3211(6)	53(2)
S(1A)	-239(6)	2322(2)	4976(6)	43(2)
O(1A)	-649(16)	1969(4)	4518(15)	61(5)
O(2A)	-268(15)	2404(3)	6206(12)	47(4)
N(1A)	2444(13)	2983(4)	3672(12)	27(3)
N(2A)	1309(15)	2430(4)	4832(14)	30(3)
N(3A)	-9(14)	3131(4)	4699(13)	25(3)
C(1A)	737(18)	2571(5)	2260(16)	24(3)
C(2A)	1126(16)	2913(6)	2631(14)	23(3)
C(3A)	283(17)	3187(5)	2057(16)	24(3)
C(4A)	-1073(18)	3128(5)	1073(16)	26(3)
C(5A)	-2962(18)	2707(5)	-182(18)	37(3)
C(6A)	-3473(19)	2373(5)	-478(18)	40(3)
C(7A)	-2544(18)	2100(6)	141(18)	39(3)
C(8A)	-1184(18)	2159(5)	983(18)	34(3)
C(9A)	-622(17)	2501(5)	1356(16)	24(3)
C(10A)	-1560(17)	2783(5)	759(17)	26(3)
C(11A)	1786(19)	2282(5)	2877(18)	30(3)
C(12A)	2080(19)	2225(5)	4155(17)	34(3)
C(13A)	3027(21)	1942(5)	4782(20)	45(4)
C(14A)	3806(22)	1761(5)	4136(21)	48(4)
C(15A)	4478(23)	1631(6)	2258(21)	50(4)
C(16A)	4340(23)	1691(6)	1108(22)	53(4)
C(17A)	3284(21)	1926(5)	449(21)	49(4)
C(18A)	2425(20)	2128(5)	990(21)	40(3)
C(19A)	2576(20)	2083(5)	2206(19)	35(3)
C(20A)	3593(22)	1806(5)	2871(21)	45(3)
C(22A)	-19(20)	3485(5)	4683(18)	34(3)
C(23A)	-1279(19)	3694(5)	4061(18)	36(3)
C(24A)	-2558(21)	3539(5)	3408(18)	38(3)
C(25A)	-4006(20)	3004(5)	2641(18)	44(3)
C(26A)	-4121(22)	2651(6)	2607(20)	48(4)
C(27A)	-2939(22)	2455(6)	3259(20)	44(4)
C(28A)	-1621(18)	2611(5)	4025(17)	30(3)
C(29A)	-1418(18)	2977(5)	4031(15)	30(3)
C(30A)	-2676(20)	3178(5)	3351(18)	36(3)
C(31A)	4594(21)	3036(6)	6252(19)	42(4)
C(32A)	3767(19)	3341(6)	6420(17)	35(3)
C(33A)	2714(19)	3298(6)	7065(18)	35(3)
C(34A)	2403(17)	2950(7)	7527(15)	34(3)
C(35A)	3202(20)	2671(6)	7261(18)	40(4)
C(36A)	4379(20)	2721(6)	6719(18)	43(4)
C(37A)	5767(20)	3071(6)	5596(19)	60(6)
C(38A)	1349(17)	2930(7)	8277(15)	39(3)
C(39A)	2242(21)	3039(6)	9614(18)	50(5)
C(40A)	-86(22)	3141(6)	7818(21)	63(5)
Ru(1B)	3180(2)	4982(1)	4447(1)	26(1)
Cl(1B)	1816(5)	4168(1)	6727(6)	49(2)
S(1B)	5620(6)	5580(2)	4975(5)	36(2)
O(1B)	6038(15)	5929(3)	5411(15)	50(4)
O(2B)	5686(14)	5496(4)	3774(13)	52(4)
N(1B)	2939(13)	4913(4)	6275(12)	22(3)
N(2B)	4067(15)	5470(4)	5128(14)	24(3)
N(3B)	5425(15)	4766(4)	5284(14)	25(3)
C(1B)	4619(18)	5330(5)	7671(17)	25(3)
C(2B)	4251(15)	5002(5)	7341(15)	22(3)
C(3B)	5177(17)	4716(5)	8001(17)	28(3)
C(4B)	6452(17)	4771(5)	8881(17)	28(3)
C(5B)	8366(19)	5202(5)	10176(18)	39(3)
C(6B)	8775(19)	5539(6)	10427(19)	44(4)
C(7B)	7860(19)	5814(6)	9759(18)	43(4)
C(8B)	6526(19)	5752(5)	8932(18)	34(3)



Table 5 (Continued)

C(9B)	6030(18)	5404(5)	8651(17)	29(3)
C(10B)	6912(17)	5118(5)	9252(17)	26(3)
C(11B)	3525(18)	5626(5)	7026(17)	28(3)
C(12B)	3370(18)	5683(5)	5817(17)	28(3)
C(13B)	2358(19)	5937(5)	5224(19)	35(3)
C(14B)	1559(20)	6148(5)	5758(18)	35(3)
C(15B)	850(22)	6277(5)	7639(20)	42(3)
C(16B)	1059(22)	6215(6)	8865(21)	50(4)
C(17B)	2078(21)	5955(5)	9538(20)	42(3)
C(18B)	2950(20)	5770(5)	8998(19)	39(3)
C(19B)	2746(20)	5824(5)	7674(18)	30(3)
C(20B)	1695(20)	6083(5)	7017(19)	34(3)
C(22B)	5410(20)	4411(5)	5302(18)	35(3)
C(23B)	6622(20)	4199(6)	5897(19)	38(3)
C(24B)	7946(21)	4345(5)	6533(19)	41(3)
C(25B)	9419(19)	4871(5)	7366(17)	37(3)
C(26B)	9531(20)	5226(6)	7424(19)	43(4)
C(27B)	8332(19)	5438(6)	6692(19)	36(3)
C(28B)	7030(17)	5296(5)	5954(17)	27(3)
C(29B)	6768(17)	4918(5)	5899(15)	26(3)
C(30B)	8055(19)	4729(5)	6623(18)	32(3)
C(31B)	717(20)	4858(5)	3681(18)	31(3)
C(32B)	1546(19)	4583(5)	3444(17)	31(3)
C(33B)	2647(19)	4608(5)	2903(17)	29(3)
C(34B)	2963(17)	4932(5)	2447(15)	26(3)
C(35B)	2154(18)	5229(5)	2647(17)	30(3)
C(36B)	1030(19)	5195(5)	3296(18)	32(3)
C(37B)	−472(19)	4819(5)	4286(19)	47(5)
C(38B)	4059(17)	4961(7)	1721(16)	38(3)
C(39B)	3142(21)	4887(6)	336(18)	47(5)
C(40B)	5466(19)	4758(6)	2190(20)	57(5)
N(1S)	−5656(33)	1640(8)	−2098(26)	104(8)
N(2S)	−3300(31)	3701(8)	−1457(32)	125(10)
N(3S)	−1352(28)	4199(8)	1349(23)	105(8)
N(4S)	978(29)	6243(8)	2072(23)	97(7)
C(1S)	−6372(43)	1414(10)	−2408(33)	95(8)
C(2S)	−7494(36)	1162(8)	−2978(29)	113(9)
C(3S)	−4130(42)	3797(9)	−881(38)	108(9)
C(4S)	−5042(34)	3906(8)	−236(31)	106(9)
C(5S)	−532(40)	4107(10)	812(31)	102(8)
C(6S)	513(31)	3990(8)	213(27)	101(8)
C(7S)	1427(37)	6498(9)	2380(29)	83(7)
C(8S)	2247(32)	6839(7)	2836(27)	101(8)

$U_{eq}$  is defined as one third of the trace of the orthogonalized  $U_{ij}$  tensor.

The crystals of **5** and **6** were transferred to a Siemens SMART/CCD three circle ( $\chi$  fixed at  $54.65^\circ$ ) diffractometer equipped with a cold stream of  $N_2$  gas and a graphite-monochromated  $Mo-K_\alpha$  radiation source. Data collection was performed at  $-60^\circ C$  with an X-ray power of 2.2 kW. A total of 1321 frames of two-dimensional diffraction images were collected, each of which was measured for 10 s. Crystallographic data for **5** and **6** are summarized in Tables 1 and 4, respectively.

The raw data frames were processed to produce conventional intensity data by the program SAINT. An initial background was determined from the first  $12^\circ$  of data. Integration was performed with constant spot sizes of  $1.75^\circ$  in the detector plane and  $0.9^\circ$  in omega.

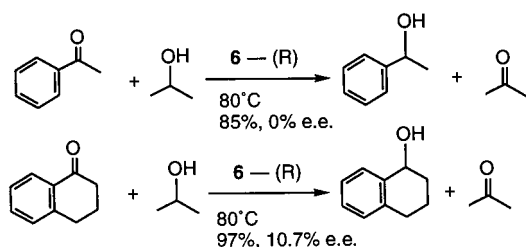
Table 6

Selected bond lengths (Å) and angles ( $^\circ$ ) for **6**

Ru(1A)–N(2A)	2.10(2)	Ru(1A)–N(3A)	2.125(14)
Ru(1A)–C(35A)	2.15(2)	Ru(1A)–C(31A)	2.17(2)
Ru(1A)–N(1A)	2.194(12)	Ru(1A)–C(32A)	2.20(2)
Ru(1A)–C(36A)	2.21(2)	Ru(1A)–C(33A)	2.22(2)
Ru(1A)–C(34A)	2.26(2)	S(1A)–O(2A)	1.449(13)
S(1A)–O(1A)	1.46(2)	S(1A)–N(2A)	1.555(14)
S(1A)–C(28A)	1.78(2)	N(1A)–C(2A)	1.44(2)
N(2A)–C(12A)	1.44(2)	N(3A)–C(22A)	1.35(2)
N(3A)–C(29A)	1.42(2)	C(1A)–C(2A)	1.39(2)
C(1A)–C(9A)	1.39(2)	C(1A)–C(11A)	1.50(2)
C(2A)–C(3A)	1.35(2)	C(3A)–C(4A)	1.42(2)
C(4A)–C(10A)	1.40(2)	C(5A)–C(6A)	1.37(3)
C(5A)–C(10A)	1.44(2)	C(6A)–C(7A)	1.40(3)
C(7A)–C(8A)	1.35(2)	C(8A)–C(9A)	1.42(2)
C(9A)–C(10A)	1.42(2)	C(11A)–C(12A)	1.41(2)
C(11A)–C(19A)	1.44(2)	C(12A)–C(13A)	1.44(2)
C(13A)–C(14A)	1.37(3)	C(14A)–C(20A)	1.41(3)
C(15A)–C(16A)	1.30(3)	C(15A)–C(20A)	1.40(2)
C(16A)–C(17A)	1.37(3)	C(17A)–C(18A)	1.39(2)
C(18A)–C(19A)	1.36(3)	C(19A)–C(20A)	1.47(3)
C(22A)–C(23A)	1.41(2)	C(23A)–C(24A)	1.33(3)
C(24A)–C(30A)	1.39(3)	C(25A)–C(26A)	1.35(3)
C(25A)–C(30A)	1.41(3)	C(26A)–C(27A)	1.35(3)
C(27A)–C(28A)	1.40(3)	C(28A)–C(29A)	1.41(3)
C(29A)–C(30A)	1.41(3)	C(31A)–C(36A)	1.36(3)
C(31A)–C(32A)	1.44(3)	C(31A)–C(37A)	1.51(2)
C(32A)–C(33A)	1.41(2)	C(33A)–C(34A)	1.49(3)
C(34A)–C(35A)	1.39(3)	C(34A)–C(38A)	1.49(2)
C(35A)–C(36A)	1.43(2)	C(38A)–C(40A)	1.51(3)
C(38A)–C(39A)	1.55(3)		
N(2A)–Ru(1A)–N(3A)	88.0(5)	N(2A)–Ru(1A)–C(35A)	87.2(7)
N(3A)–Ru(1A)–C(35A)	130.8(6)	N(2A)–Ru(1A)–C(31A)	124.2(7)
N(3A)–Ru(1A)–C(31A)	145.8(7)	C(35A)–Ru(1A)–C(31A)	68.3(8)
N(2A)–Ru(1A)–N(1A)	83.8(6)	N(3A)–Ru(1A)–N(1A)	85.4(5)
C(35A)–Ru(1A)–N(1A)	142.4(6)	C(31A)–Ru(1A)–N(1A)	87.0(6)
N(2A)–Ru(1A)–C(32A)	162.3(7)	N(3A)–Ru(1A)–C(32A)	109.6(6)
C(35A)–Ru(1A)–C(32A)	81.5(8)	C(31A)–Ru(1A)–C(32A)	38.5(7)
N(1A)–Ru(1A)–C(32A)	96.9(6)	N(2A)–Ru(1A)–C(36A)	95.7(7)
N(3A)–Ru(1A)–C(36A)	167.8(6)	C(35A)–Ru(1A)–C(36A)	38.3(6)
C(31A)–Ru(1A)–C(36A)	36.1(7)	N(1A)–Ru(1A)–C(36A)	106.5(6)
C(32A)–Ru(1A)–C(36A)	67.1(8)	N(2A)–Ru(1A)–C(33A)	146.9(6)
N(3A)–Ru(1A)–C(33A)	92.3(6)	C(35A)–Ru(1A)–C(33A)	67.7(8)
C(31A)–Ru(1A)–C(33A)	67.4(7)	N(1A)–Ru(1A)–C(33A)	129.3(7)
C(32A)–Ru(1A)–C(33A)	37.1(6)	C(36A)–Ru(1A)–C(33A)	78.2(7)
N(2A)–Ru(1A)–C(34A)	108.6(7)	N(3A)–Ru(1A)–C(34A)	100.8(6)
C(35A)–Ru(1A)–C(34A)	36.6(7)	C(31A)–Ru(1A)–C(34A)	80.8(7)
N(1A)–Ru(1A)–C(34A)	166.1(7)	C(32A)–Ru(1A)–C(34A)	69.4(7)
C(36A)–Ru(1A)–C(34A)	66.9(6)	C(33A)–Ru(1A)–C(34A)	38.9(7)
O(2A)–S(1A)–O(1A)	117.8(8)	O(2A)–S(1A)–N(2A)	110.1(8)
O(1A)–S(1A)–N(2A)	110.9(8)	O(2A)–S(1A)–C(28A)	103.1(8)
O(1A)–S(1A)–C(28A)	107.4(9)	N(2A)–S(1A)–C(28A)	106.6(8)
C(2A)–N(1A)–Ru(1A)	116.8(8)	C(12A)–N(2A)–S(1A)	123.0(13)
C(12A)–N(2A)–Ru(1A)	118.8(10)	S(1A)–N(2A)–Ru(1A)	117.9(8)
C(22A)–N(3A)–C(29A)	114(2)	C(22A)–N(3A)–Ru(1A)	112.7(11)
C(29A)–N(3A)–Ru(1A)	132.6(12)	C(2A)–C(1A)–C(9A)	120(2)
C(2A)–C(1A)–C(11A)	119(2)	C(9A)–C(1A)–C(11A)	121(2)
C(3A)–C(2A)–C(1A)	122(2)	C(3A)–C(2A)–N(1A)	118(2)
C(1A)–C(2A)–N(1A)	120(2)	C(2A)–C(3A)–C(4A)	120(2)
C(10A)–C(4A)–C(3A)	119(2)	C(6A)–C(5A)–C(10A)	123(2)
C(5A)–C(6A)–C(7A)	117(2)	C(8A)–C(7A)–C(6A)	122(2)
C(7A)–C(8A)–C(9A)	123(2)	C(1A)–C(9A)–C(10A)	119(2)
C(1A)–C(9A)–C(8A)	125(2)	C(10A)–C(9A)–C(8A)	116(2)
C(4A)–C(10A)–C(9A)	119(2)	C(4A)–C(10A)–C(5A)	122(2)
C(9A)–C(10A)–C(5A)	119(2)	C(12A)–C(11A)–C(19A)	120(2)

Table 6 (Continued)

C(12A)–C(11A)–C(1A)	119(2)	C(19A)–C(11A)–C(1A)	121(2)
C(11A)–C(12A)–C(13A)	122(2)	C(11A)–C(12A)–N(2A)	120(2)
C(13A)–C(12A)–N(2A)	118(2)	C(14A)–C(13A)–C(12A)	117(2)
C(13A)–C(14A)–C(20A)	124(2)	C(16A)–C(15A)–C(20A)	122(2)
C(15A)–C(16A)–C(17A)	120(2)	C(16A)–C(17A)–C(18A)	122(2)
C(19A)–C(18A)–C(17A)	120(2)	C(18A)–C(19A)–C(11A)	125(2)
C(18A)–C(19A)–C(20A)	118(2)	C(11A)–C(19A)–C(20A)	118(2)
C(15A)–C(20A)–C(14A)	123(2)	C(15A)–C(20A)–C(19A)	118(2)
C(14A)–C(20A)–C(19A)	119(2)	N(3A)–C(22A)–C(23A)	125(2)
C(24A)–C(23A)–C(22A)	119(2)	C(23A)–C(24A)–C(30A)	121(2)
C(26A)–C(25A)–C(30A)	122(2)	C(27A)–C(26A)–C(25A)	120(2)
C(26A)–C(27A)–C(28A)	121(2)	C(27A)–C(28A)–C(29A)	121(2)
C(27A)–C(28A)–S(1A)	116(2)	C(29A)–C(28A)–S(1A)	122.8(13)
C(30A)–C(29A)–C(28A)	117(2)	C(30A)–C(29A)–N(3A)	122(2)
C(28A)–C(29A)–N(3A)	121(2)	C(24A)–C(30A)–C(29A)	119(2)
C(24A)–C(30A)–C(25A)	123(2)	C(29A)–C(30A)–C(25A)	119(2)
C(36A)–C(31A)–C(32A)	121(2)	C(36A)–C(31A)–C(37A)	120(2)
C(32A)–C(31A)–C(37A)	120(2)	C(36A)–C(31A)–Ru(1A)	73.4(13)
C(32A)–C(31A)–Ru(1A)	72.0(11)	C(37A)–C(31A)–Ru(1A)	129.7(14)
C(33A)–C(32A)–C(31A)	118(2)	C(33A)–C(32A)–Ru(1A)	72.2(10)
C(31A)–C(32A)–Ru(1A)	69.5(12)	C(32A)–C(33A)–C(34A)	122(2)
C(332A)–C(33A)–Ru(1A)	70.7(10)	C(34A)–C(33A)–Ru(1A)	71.7(10)
C(35A)–C(34A)–C(38A)	125(2)	C(35A)–C(34A)–C(33A)	116(2)
C(38A)–C(34A)–C(33A)	119(2)	C(35A)–C(34A)–Ru(1A)	67.6(10)
C(38A)–C(34A)–Ru(1A)	136.3(12)	C(33A)–C(34A)–Ru(1A)	69.3(10)
C(34A)–C(35A)–C(36A)	122(2)	C(34A)–C(35A)–Ru(1A)	75.8(11)
C(36A)–C(35A)–Ru(1A)	73.0(11)	C(31A)–C(36A)–C(35A)	121(2)
C(31A)–C(36A)–Ru(1A)	70.5(13)	C(35A)–C(36A)–Ru(1A)	68.7(10)
C(34A)–C(38A)–C(40A)	116(2)	C(34A)–C(38A)–C(39A)	107.8(14)
C(40A)–C(38A)–C(39A)	110(2)		

Scheme 4. Asymmetric transfer hydrogenations by ruthenium complex **6**.

The intensity data were corrected for Lorentz, polarization effects, and absorption corrections.

#### 4.7. Solution and refinement of structures **5** and **6**

The structures were solved by direct methods and standard difference Fourier techniques. Two independent molecules were found in the asymmetric unit cell. All final refinements were completed using SHELXL-93. This was carried out on  $F^2$  for all reflections except for those with either very negative  $F$  or reflections flagged for potential systematic errors, normally for reflections besides strong ones. Final non-hydrogen

atom atomic positional and equivalent isotropic thermal parameters, selected bond distances and angles for **5** and **6** are provided in Tables 2, 3, 5 and 6. Final anisotropic temperature factors and hydrogen positional parameters are given in Tables S1–S5.

### 5. Supplementary material

Tables of atom coordinates, anisotropic thermal parameters of **5** and **6** (22 pages) are available from the author (L.C.).

### Acknowledgements

We are grateful to The University of Illinois at Chicago for financial support.

### References

- [1] R. Noyori, *Asymmetric Catalysis in Organic Synthesis*, Wiley, New York, 1994, Chapter 2.
- [2] (a) J.B. Jones, *Tetrahedron* 42 (1986) 3351. (b) E. Schoffers, A. Golebiowski, C.R. Johnson, *Tetrahedron* 52 (1996) 3769.
- [3] (a) G. Zassinovich, G. Mestroni, S. Gladioli, *Chem. Rev.* 92 (1992) 1051. (b) C.F. de Graauw, J.A. Peters, H. van Bekkum, J. Huskens, *J. Synth.* (1994) 1007.
- [4] (a) M. Saburi, M. Ohnuki, M. Ogasawara, T. Takahashi, Y. Uchida, *Tetrahedron Lett.* 33 (1992) 5783. (b) W. Leitner, J.M. Brown, H.J. Brunner, *J. Am. Chem. Soc.* 115 (1993) 152. (c) R. Noyori, S. Hashiguchi, *Acc. Chem. Res.* 30 (1997) 97.
- [5] (a) I. Ojima (Ed.) *Catalytic Asymmetric Synthesis*, VCH, New York, 1993. (b) R. Noyori, *Asymmetric Catalysis in Organic Synthesis*, Wiley, New York, 1994.
- [6] (a) K. Kabuto, T. Yoshida, S. Yamaguchi, S. Miyano, H. Hashimoto, *J. Org. Chem.* 50 (1985) 3013. (b) C.-W. Ho, W.-C. Cheng, M.-C. Cheng, S.-M. Peng, K.-F. Cheng, C.-M. Che, *J. Chem. Soc. Dalton Trans.* (1996) 405. (c) E.M. Carreira, R.A. Singer, W.J. Lee, *J. Am. Chem. Soc.* 116 (1994) 8837. (d) J.-H. Lin, C.-M. Che, T.-F. Lai, C.-K. Poon, Y.X. Cui, *J. Chem. Soc. Chem. Commun.* (1991) 468.
- [7] (a) K. Kabuto, T. Yoshida, S. Yamaguchi, S. Miyano, H.J. Hashimoto, *Org. Chem.* 50 (1985) 3013. (b) C.-W. Ho, W.-C. Cheng, M.-C. Cheng, S.-M. Peng, K.-F. Cheng, C.-M. Che, *J. Chem. Soc. Dalton Trans.* (1996) 405. (c) E.M. Carreira, R.A. Singer, W. Lee, *J. Am. Chem. Soc.* 116 (1994) 8837. (d) J.-H. Lin, C.-M. Che, T.-F. Lai, C.-K. Poon, Y.X. Cui, *J. Chem. Soc. Chem. Commun.* (1991) 468.
- [8] Y. Han, L. Cai, *Tetrahedron Lett.* 38 (1997) 5423–5426.
- [9] K.K. Andersen, *Sulphonic acids and their derivatives*, in: D.H.R. Barton, W.D. Ollis (Eds.), *Comprehensive Organic Chemistry*, vol. 3, Pergamon Press, Oxford, 1979.
- [10] H. Mahmoud, Y. Han, B.M. Segal, L. Cai, *Tetrahedron Asymmetry* 9 (1998) 2035.
- [11] K.-J. Haaack, S. Hashiguchi, A. Fujii, T. Ikariya, R. Noyori, *Angew. Chem. Int. Ed. Engl.* 36 (1997) 285.
- [12] L. Cai, Y. Han, unpublished results.